Electronic and magnetic structure of Fe_3S_4: GGA+U investigation

A. J. Devey,* R. Grau-Crespo, and N. H. de Leeuw
Department of Chemistry, University College, University of London, 20 Gordon Street, London WC1H 0AJ, United Kingdom
(Received 10 February 2009; revised manuscript received 18 March 2009; published 26 May 2009)

The electronic and magnetic behavior of the iron sulphide mineral greigite (Fe_3S_4) is studied using *ab initio* density-functional theory in the generalized gradient approximation (GGA) with the on-site Hubbard U_{eff} parameter (GGA+U). The effect of the Hubbard correction is investigated and is found to be a necessary requirement for the accurate description of both the unit cell structure and the magnetic moment. A ferrimagnetic normal-spinel structure is found when $U_{eff}=0$ eV, while for all values of $U_{eff}>0$ eV an inverse spinel structure is predicted, in agreement with experiment. For low values of U_{eff} ($0<U_{eff}<4$ eV) the predicted electronic structure corresponds to that of a semimetal, with semimetallicity arising from electron hopping between ferric and ferrous Fe on octahedral sites. For values of $U_{eff}\geq 4$ eV the S atoms are found to oxidize the ferrous octahedral sites Fe to the ferric state. To determine whether GGA+U predicts a stable monoclinic form of greigite arising from a Verwey-type low-temperature transition, analogous to that seen in magnetite, a monoclinic form of greigite is postulated. It is found that such a phase is stable, with an electronic band-gap opening up for values of $U_{eff}\geq 2$ eV, but is energetically unfavorable when compared with the spinel phase for all U_{eff} values tested. It is argued that an accurate description of all the properties of greigite requires a U_{eff} value of approximately 1 eV.

DOI: 10.1103/PhysRevB.79.195126 PACS number(s): 71.20.−b, 71.15.Mb, 71.27.+a, 71.28.+d

I. INTRODUCTION

Greigite (Fe_3S_4) is the sulphide counterpart of the well-known iron oxide spinel magnetite.[1] First defined as a mineral by Skinner *et al.*[2] from a Californian lacustrine sediment sequence, it is now considered a common magnetic material[3] and has been found in many natural environments with ages up to several million years old.[4] Research has suggested that greigite may have played an important role as a catalyst in the development of protometabolism, primarily due to its similarity to the cubane cluster structure Fe_4S_4,[5] which is still found as the active sites in many enzymes.[6] In addition, greigite has been discovered in the scales of a deep sea hydrothermal vent gastropod,[7] it is an important paleomagnetic material[1] and is widespread in magnetostatic bacteria.[8] Greigite is believed to form from mackinawite ($Fe^{2+}S^{2-}$) via oxidation of two-thirds of the Fe^{2+} cations, together with rearrangement about the cubic close-packed S anion sublattice[9] which in turn undergoes a small volume reduction of around 12%.[10] Recently, both one-dimensional rods[11] and two-dimensional nanosheets[12] of greigite have been synthesized, opening up the possibility of research into the magnetic properties of low-dimensional iron sulphide structures.

Greigite has a cubic unit cell containing 8 iron cations in tetrahedral coordination (hereafter referred to as *A* sites) and 16 iron cations in octahedral coordination (*B* sites) with 32 sulfur anions (Fig. 1).[13] The magnetic moments on the tetrahedral and octahedral Fe sublattice are aligned in an antiparallel fashion, rendering greigite ferrimagnetic.[14]

Measurements of the magnetization via high-field experiments at room temperature give a saturation magnetization for greigite of 3.13 μ_B per formula unit (f.u.), which at 5 K increases to 3.35 μ_B/f.u. due to decreased thermal excitation.[15] This recent result is in contrast to the previously determined experimental value of 2.2 (± 0.3) μ_B/f.u.,[14] presumed to be due to the presence of impurities, vacancies or a combination of both in the greigite samples tested. In any case, the magnetization of greigite is below the value of ~4.0 μ_B/f.u. observed in magnetite,[16] which is the value expected from a purely ionic model (4 μ_B on Fe^{2+}; 5 μ_B on Fe^{3+}). Mössbauer measurements performed on both natural and synthetic greigite samples[14,17–20] have demonstrated that the cations on the tetrahedral and octahedral sublattices order with an inverse spinel structure, $(Fe^{3+})_A(Fe^{2+}Fe^{3+})_BS$, down to a temperature of at least 4.2 K. Recent measurements have suggested an estimate for the J_{AB} exchange constant between tetrahedral and octahedral sublattices in greigite of ~1.03 meV,[15] lower than that calculated for magnetite (2.88 meV),[21] indicating a lower level of magnetic coupling in the sulfide.

Spender *et al.*[14] carried out measurements of the conductivity of greigite and found the presence of delocalized

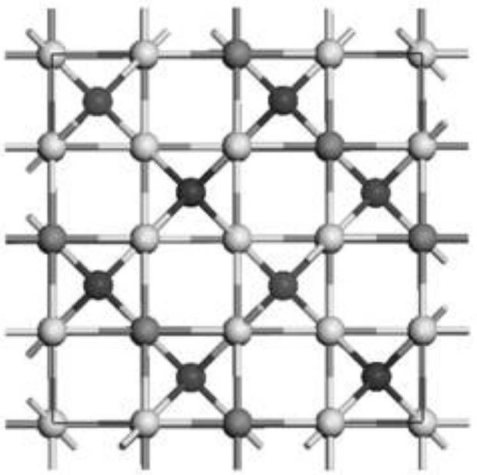

FIG. 1. Structure of greigite viewed along the ⟨100⟩ axis. The S atoms are shown in white, the tetrahedral Fe in dark gray, and the octahedral Fe in light gray.

charge carriers in the compound, which they attributed to electron hopping between ferrous and ferric Fe on octahedral sites, leading to a semimetallic nature. Regarding the electronic structure of greigite, two band schemes have been proposed: The first suggests that greigite possesses an average of ferric (d^5) and ferrous (d^6) iron on B sites, similar to that found in magnetite;[22] while the second assumes that ferric iron on the B sites is reduced by the sulfur anions and thus only ferrous iron is present in octahedral coordination.

Experimental low-temperature magnetization measurements have failed to reach a consensus regarding the existence of a Verwey-type transition in greigite at temperatures between 4.2 and 300 K, and it is not clear whether a transition would be discernable using such methods. While some studies have not detected a transition,[23–25] it has been pointed out that the greigite samples tested may not be sufficiently stoichiometric for the transition to be apparent, possibly due to the presence of B site vacancies. A maximum in remnant saturation magnetization measured at 10 K for a variety of both synthetic and natural greigite samples has been suggested as evidence of a transition, although other mechanisms may be responsible which are unconnected with any transition.[4]

A number of questions remain unanswered in relation to the electronic structure and magnetic behavior of greigite that are well suited to an investigation by modern *ab initio* techniques. The main aim of this work is to investigate the electronic structure of greigite. Similar to the findings of studies into magnetite,[26,27] the importance of the on-site Fe electronic correlation represented by the U_{eff} parameter in the description of greigite will be investigated. Finally, we explore the possibility of any low-temperature Verwey-type transition in greigite.

II. METHODOLOGY

The greigite structure is modeled using the Vienna *ab initio* simulation program (VASP),[28–31] which employs spin-polarized density-functional theory (DFT) with a basis set constructed from plane waves. The theory and application of the plane-wave DFT methodology have been described extensively elsewhere;[32] it is well established and has been applied to a wide range of materials including transition metal sulphides,[33–35] oxides[36–38] and spinels.[27,39] All calculations are performed within the generalized gradient approximation (GGA), using the exchange-correlation functional developed by Perdew *et al.*[40] and the spin interpolation formula of Vosko *et al.*[41] The interaction between the valence electrons and the core is described with the projector augmented wave (PAW) method[42] in the implementation of Kresse and Joubert.[43] The core levels, which are kept frozen during the calculations, consisted of orbitals up to, and including, the $3p$ levels for Fe and the $2p$ level for S. Geometry optimization of the 56-atom cubic unit cell is performed with an energy cutoff of 600 eV and a Monkhorst-Pack (MP)[44] grid of $4\times4\times4$, while the 56-atom monoclinic unit cell used the same cutoff energy and a MP grid of $4\times4\times2$. This high value for the cutoff energy ensured that no Pulay stresses occurred within the cell during relaxations. In order to improve the convergence of the Brillouin-zone integrations, the partial occupancies were determined using Gaussian smearing, with a set width for all calculations of 0.02 eV. These smearing techniques can be considered in the form of a finite-temperature DFT,[45] where the variational quantity is the electronic free energy. The optimization of the structures was conducted via a conjugate gradients technique, which uses the total energy and the Hellmann-Feynman forces on the atoms. Spin-orbit coupling was not taken into account.

It has been pointed out in several studies of transition metal compounds[46–48] that the GGA methodology often provides an unsatisfactory description of such highly correlated materials. Thus we have also performed calculations using the so-called GGA+U method, in the formulation of Lichtenstein[49] and later Dudarev,[50] where a single parameter, U_{eff}, determines an orbital-dependent correction to the GGA energy,

$$E_{GGA+U} = E_{GGA} + U_{eff}\sum_{\sigma} \mathrm{Tr}[\rho^{\sigma} - \rho^{\sigma}\rho^{\sigma}], \quad (1)$$

where ρ^{σ} is the on-site density matrix with spin component σ. The parameter U_{eff} is generally expressed as the difference between two parameters, the Hubbard U, which is the Coulomb-energetic cost to place two electrons at the same site, and an approximation of Hund's exchange parameter J, which is almost constant at ~ 1 eV.[51] The GGA+U correction alters the one-electron potential locally for the specified orbitals, here the Fe d orbitals, reducing the hybridization with the S ligands. The $U_{eff}=0$ case represents the GGA limit. Details of the implementation of the GGA+U method in the VASP code can be found in the work of Rohrbach *et al.*,[34] where it was also shown that although the U_{eff} parameter introduces a form of semiempiricism into the calculations, the Hubbard correction improves the description of many transition metal sulphides. It was also instrumental in the description of the low-temperature magnetite structure.[26] The U_{eff} method is chosen over other exchange functional methods such as hybrid functionals due to the large system size. A useful comparison of GGA+U with the hybrid functional B3LYP for the antiferromagnetic material $FeSbO_4$ is given in Ref. 38. Work is ongoing regarding improvements in both the GGA[52] and hybrid methods.[53]

The greigite spinel structure determined by Uda[13] is used as the starting geometric arrangement, and a full relaxation of the unit cell volume, shape, and internal atomic coordinates is undertaken, followed by a second relaxation solely of the internal coordinates in order to ensure full relaxation of the structure. Finally, a single-point calculation of the electronic structure is completed, using a tetrahedral smearing method with Blochl corrections in order to obtain the electronic ground state and the electronic density of states.

III. RESULTS

A. Spinel structure

The 56-atom cubic unit cell of greigite is modeled using GGA+U calculations for a range of U_{eff} values and three different initial magnetic arrangements: nonmagnetic (zero

initial magnetic moments on all Fe sites); inverse spinel (initial magnetic moments of 5 μ_B on each of the tetrahedral Fe sites and 4.5 μ_B on each of the 16 octahedral sites); and normal-spinel (initial magnetic moments of 4 μ_B on each of the tetrahedral sites and 5 μ_B on each of the octahedral sites). For U_{eff}=0 eV, the VASP calculation of the greigite spinel structure gives a cubic structure with lattice parameter a=9.48 Å. It was found that the resulting magnetic structure is always ferrimagnetic with a magnetization per formula unit of 2.08 μ_B, regardless of the initial arrangement of the magnetic moments. These results show only moderate agreement with the experimentally determined values for greigite; a=9.88 Å and 3.35 μ_B for the lattice parameters and magnetic moment per formula unit respectively.[13,15]

In order to determine whether the introduction of the Hubbard parameter improves the DFT description of greigite, suitable values for the U_{eff} parameter are applied. Identical cell relaxations as for the U_{eff}=0 eV case are undertaken. The U_{eff} values chosen vary from 0.5 to 5 eV, in steps of 0.5 eV.

The cubic unit cell is accurately reproduced for all cases, with $a=b=c$ and angles at 90°. The initial magnetic moment was found to be inconsequential, with all three cases converging to a stable ferrimagnetic state for each U_{eff} value tested. The calculated lattice parameters for each value of U_{eff} are shown in Fig. 2(a). The introduction of the U_{eff} value has a significant effect upon the lattice parameters, compensating for the overbinding seen in the U_{eff}=0 eV case and yielding the experimentally determined value for the lattice parameter at a U_{eff} of between 1 and 1.5 eV. It is worth noting that this value is similar to the value of U_{eff} found to give an accurate description of troilite (FeS).[34] The experimental value for the S u parameter of 0.2505, which represents the first internal S coordinate within the unit cell, is well reproduced for all U_{eff} values.

A plot of the magnetization per formula unit versus U_{eff} for the spinel structure is given in Fig. 2(b), and a plot of the magnitude of each individual magnetic moment from each sublattice is shown in Fig. 2(c). The magnetic moment on each site is found using a Bader analysis, where the electron spin density associated with each atom is integrated over the Bader volume of the atom in question.[54] The use of Bader analysis is justified by the fact that the effective radius of an ion changes with the oxidation state, and therefore it is not correct to perform the integration around a sphere of constant radius, when considering mixed-valence systems such as greigite.

The magnetic moments on the Fe atoms when U_{eff} =0 eV are much lower than the values in magnetite[16] or than would occur in the purely ionic case of integer unpaired electrons. This calculation gives a net magnetic moment per formula unit of 60% of the experimentally determined value, which arises from an overestimation of the covalency of the Fe-S bond by the pure GGA. Introducing the U_{eff} parameter leads to an increase in the total magnetic moment, caused by an underlying increase in the magnetic moments on both Fe_A and Fe_B sites. As the U_{eff} value is increased to 2 eV, the total magnetic moment reaches a maximum of 3.9 μ_B/f.u., close to the value of 4 μ_B/f.u. predicted for a purely ionic model. The magnetic moment on every Fe atom reaches a maximum

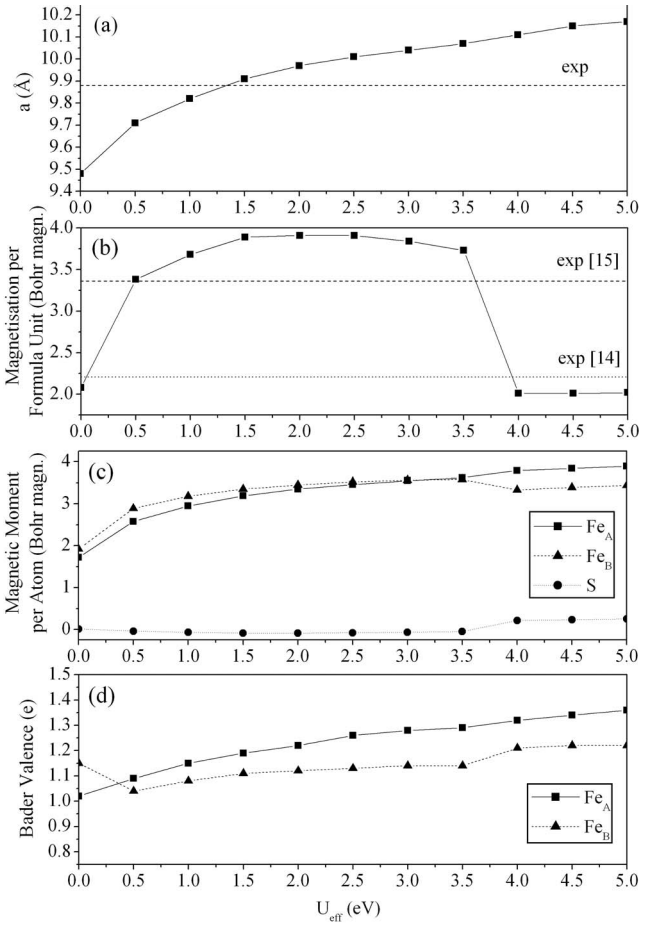

FIG. 2. (a) Calculated lattice constant for the cubic spinel structure of greigite as a function of the effective Hubbard parameter U_{eff}. The dashed line shows the experimentally determined value for a (Ref. 13). (b) Magnetization per formula unit versus U_{eff} for the spinel structure of greigite. The dashed line gives the experimental value of Chang *et al.* (Ref. 15) and the dotted line the value of Spender *et al.* (Ref. 14) (c) Magnitude of the magnetic moments on each sublattice of greigite versus U_{eff}. (d) Fe_A and Fe_B atomic Bader populations versus U_{eff} value.

of 3.6 μ_B/f.u. at U_{eff}=3.5 eV, and at this point the magnetic moments of both the tetrahedral and octahedral Fe sites are identical. From U_{eff}=4 eV upwards each S atom develops a nonzero magnetic moment of magnitude 0.2 μ_B, parallel in direction to that of the Fe_A atoms. In addition a difference of 0.45 μ_B develops between the magnetic moments of the Fe atoms on the A and B sites, with a value on the tetrahedral sites of around 3.8 μ_B and the octahedral sites of 3.3 μ_B. These two factors act to reduce the net total magnetic moment to a value of around 2.0 μ_B/f.u. for $U_{eff} \geq 4$ eV. It is noted that the experimentally determined value for the magnetic moment of 3.35 μ_B/f.u. is achieved at around U_{eff} =0.5 or 3.7 eV.

The variation in the Bader charge populations associated with the Fe_A, Fe_B, and S sites with the U_{eff} parameter is shown in Fig. 2(d). For the case of U_{eff}=0 eV, these populations indicate that there is a greater number of electrons on the Fe_A atoms than the Fe_B, corresponding to the electronic structure of a normal spinel (based on the assumption that

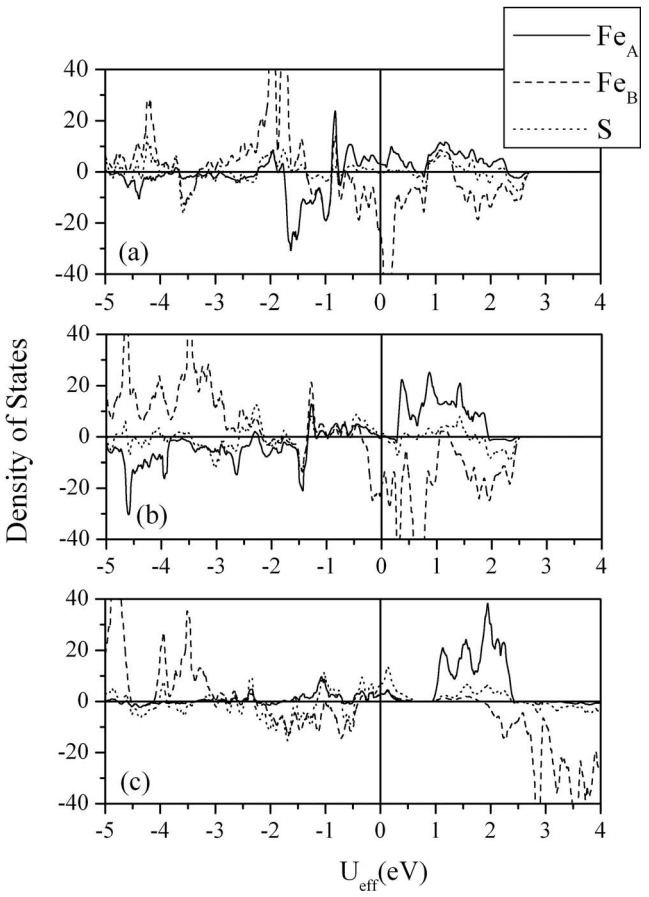

FIG. 3. Electronic DOS for the spinel form of greigite, for (a) $U_{eff}=0$ eV, (b) $U_{eff}=1$ eV, and (c) $U_{eff}=5$ eV. Contributions from each sublattice are plotted.

the greater number of electrons signifies a valence of Fe^{2+} and lesser number of electrons denotes a share of Fe^{2+} and Fe^{3+}). The introduction of the U_{eff} parameter causes the valence of the Fe_A sites to increase relative to that of the Fe_B sites, with the effect that there is a crossover of the valences of these sublattices. Thus more valence electrons are associated with the *B* sites than the *A* sites, and this relation remains for all non-zero U_{eff} values tested. Thus it can be inferred that the introduction of the U_{eff} parameter has the effect of changing the electronic structure from that of the normal spinel to that of the inverse spinel. Since it is the inverse spinel that is observed experimentally, this highlights the importance of the U_{eff} parameter in the description of greigite. Between the values of $U_{eff}=3.5$ and $U_{eff}=4$ eV, the Fe_B atoms experience a sudden reduction in Bader charge valence, and the electrons are transferred to the S atoms. This scenario corresponds to the second band picture suggested by Spender *et al.*[14]where the Fe_B are reduced by S.

Figures 3(a)–3(c) show the electronic density of states (DOS) of the spinel form of greigite for the $U_{eff}=0$, 1, and 5 eV cases, respectively. The DOS for $U_{eff}=0$ eV shows that the available states at the Fermi level arise from both the spin-down Fe_B sites and the spin-up Fe_A sites, a situation not seen for the $U_{eff}=0$ eV magnetite spinel previously modeled by Piekarz *et al.*[36] The strong effect of the U_{eff} parameter upon the Fe_A bands around the Fermi level is clearly seen in the DOS for $U_{eff}=1$ eV case [Fig. 3(b)]. A gap of 0.3 eV opens between the *e* and t_2 3*d* energy levels of the Fe_A band, while the Fe_B band is largely unaffected compared to $U_{eff}=0$ eV. This leads to a semimetallic band structure for greigite, with the spin-down Fe_B minority band providing states at the Fermi energy and a band gap in the Fe_A spin-up band. Figure 3(c) shows the DOS for $U_{eff}=5$ eV, which shows that for large U_{eff} values a splitting of the spin-down Fe_B band occurs, clearly revealing the t_{2g} and e_g energy levels of the 3*d* orbital. The Fe_B *d*-orbital spin-down band no longer occupies the energies around the Fermi level, and the semimetallic behavior disappears. The majority of states are provided by holes in the spin-up S band.

B. Monoclinic structure

Experimental investigations at low temperatures have so far been unable to provide a definitive answer as to whether a Verwey transition occurs in the greigite structure. Studies using a similar theoretical framework have proved highly successful in the description of the low-temperature monoclinic form of magnetite.[36] By analogy, a hypothetical monoclinic form of greigite is postulated, and GGA+U is used to determine its energetic stability compared to the spinel structure. The following calculations are based upon the low-temperature monoclinic structure of magnetite determined by Wright *et al.*,[55] but with the lattice parameters scaled up to account for the larger anion radius in the sulphide compared to the oxide. The scaling constant for each orthogonal lattice direction is given by the ratio of the spinel greigite lattice constant a_{grei} to that of the spinel magnetite structure a_{mag}, where $a_{grei}/a_{mag}=9.88/8.39=1.18$. Scaling each monoclinic magnetite lattice parameter by this factor gives estimates of $a=6.99$ Å, $b=6.98$ Å, and $c=19.75$ Å for the hypothetical monoclinic greigite structure. The same simulations as for the spinel structure are then repeated for a range of U_{eff} values from 0 to 5 eV, in steps of 1 eV. All relaxations yield stable monoclinic structures, with lattice parameters given in Table I.

The total magnetization per formula unit for the 56-atom monoclinic unit cell of greigite is shown in Fig. 4. For low values of U_{eff} (<4 eV), monoclinic structures with net magnetic moments of 1.7 to 2 μ_B/f.u. are found, indicating that if a transition to this structure did occur it would be accompanied by a large, observable reduction in the magnetic moment. It is noted that at low U_{eff} values, there is a splitting of the symmetry of the Fe_B sites, to the degree that the magnetic moment of half the sites is 60% greater than that of the other half. For values of $U_{eff}\geq 4$ eV, the electronic structure becomes even more complex, with four identifiable groups of four Fe_B sites, in a manner similar to the charge disproportionation seen in the low-temperature phase of magnetite. The values of the band gap for each U_{eff} value are listed in Table I. The DOSs for the monoclinic form of greigite for U_{eff} values of 0, 1, and 5 eV are shown in Figs. 5(a)–5(c), respectively. For $U_{eff}=1$ eV, both Fe_A and Fe_B sublattices provide available states at the Fermi level. As U_{eff} is increased to 1 eV a band gap opens in the Fe_B band. For $U_{eff}=5$ eV a band gap for both Fe_A and Fe_B sublattices opens

TABLE I. Calculated lattice parameters and band-gap width for the theoretical monoclinic form of greigite for a range of U_{eff}. The difference in the internal energies ΔE of the 56-atom unit cells of the spinel and monoclinic forms of greigite over the range of U_{eff} values modeled is also presented.

U_{eff} (eV)	a (Å)	b (Å)	c (Å)	Band gap (eV)	ΔE (eV)
0	6.57	6.75	18.99	0.00	1.15
1	6.79	6.87	19.52	0.00	2.69
2	6.93	6.96	19.84	0.06	3.69
3	6.96	6.99	20.02	0.16	4.55
4	7.09	7.16	20.21	0.14	2.71
5	7.29	7.24	20.61	0.29	0.92

and the structure becomes insulating, similar to that observed in simulations of monoclinic magnetite.[36]

The difference in the internal energies of the spinel and monoclinic structures for the range of U_{eff} values is given in Table I. It is clear from the calculated total energies of the two structures that the monoclinic form is only metastable with respect to the spinel. The precise energy difference between the two depends on the values of U_{eff}, but for all values the spinel structure is energetically favored.

IV. CONCLUSION

In this work we have used the GGA+U approach, where U is the on-site Hubbard U_{eff} parameter, to investigate the energetic, electronic and magnetic properties of a spinel and monoclinic structure of Fe_3S_4. Simulations of the spinel structure over the range $0 \leq U_{eff} \leq 5$ eV result in stable ferrimagnetic structures, with Fe atoms on the tetrahedral and octahedral sublattices aligned in an antiparallel manner in accord with published experimental findings. GGA in the absence of any U_{eff} correction leads to a large underestimation of the lattice parameter and the magnetic moment, as well as an electronic arrangement whereby the Bader charges of the tetrahedral and octahedral Fe sites form a normal-spinel arrangement. These errors are thought to arise from the GGA failing to take into account the electron correlation associated with the Fe atoms. The experimentally determined inverse spinel structure is correctly simulated upon the introduction of the local Coulomb interaction accounted for by U_{eff}. Small values of U_{eff}, on the order of ~ 1 eV, produce a dramatic improvement in the description of greigite, with the experimentally determined values for the lattice parameters and magnetic moments reproduced accurately. U_{eff} values greater than 3 eV produce solutions where the net magnetic moment is reduced by the occurrence of a magnetic moment on individual S atoms, antiparallel to that found on the octahedral Fe sites. This is accompanied by a decrease in the

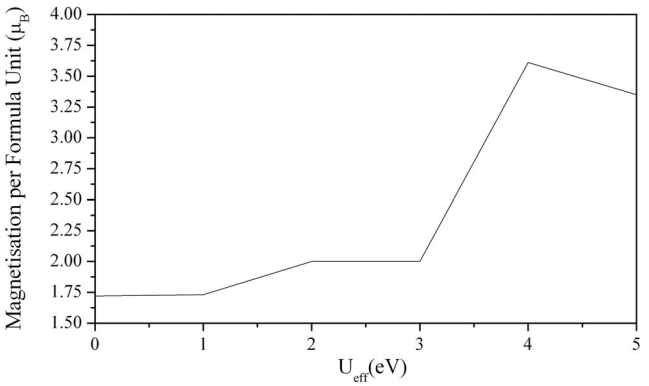

FIG. 4. Total magnetization per formula unit versus U_{eff} for the monoclinic structure of greigite.

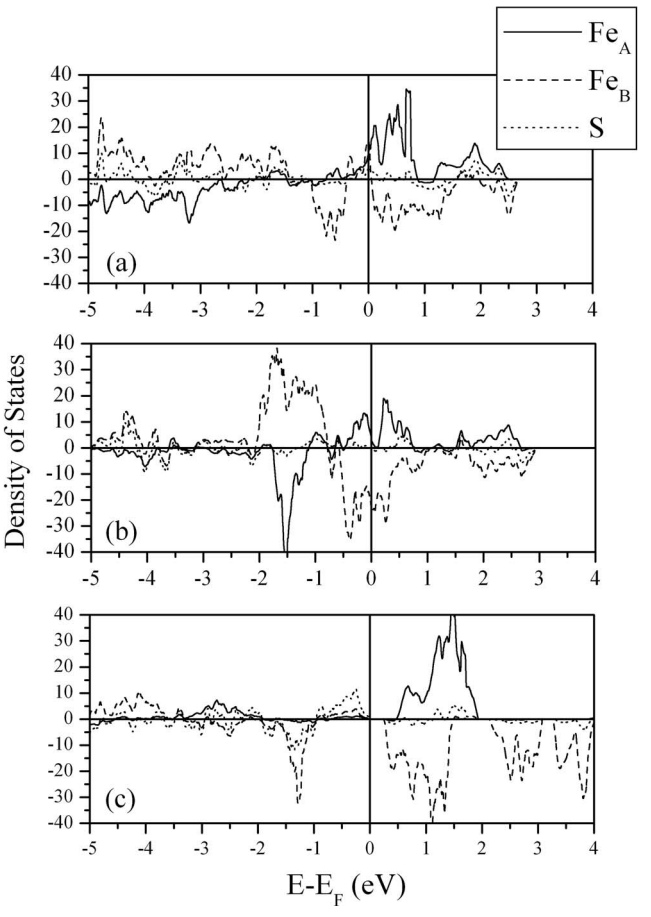

FIG. 5. DOS for the monoclinic form of greigite with (a) $U_{eff}=0$ eV, (b) $U_{eff}=1$ eV, and (c) $U_{eff}=5$ eV. Contributions from each of the sublattices are plotted.

number of electrons associated with the octahedral Fe atoms, which are transferred to the S atoms.

The two band schemes suggested by Spender *et al.*[14] for the electronic structure of greigite can now be reconsidered in the light of these results. The first scheme, where the octahedral Fe sites of greigite are occupied by a combination of ferric and ferrous iron is the scenario supported by our calculations for $U_{eff} \leq 3$ eV. The second scheme, where the S ions reduce the ferric Fe ions so that all Fe in greigite is ferrous, is seen when $U_{eff} \geq 3.5$ eV. It is not possible to discern the most correct value of U_{eff}, based only on the results presented here. However, since the experimental magnetization and the cell parameters are better reproduced at low U_{eff} values, we would suggest the use of $U_{eff}=1$ eV for the GGA+U modeling of greigite. This value is lower than that suggested for magnetite[36] but very similar to that suggested for the iron sulphide troilite.[34] This is postulated to be due to the covalent nature of the Fe-S bond being more pronounced than that of the more ionic Fe-O bond, and thus the electron correlation represented by the U_{eff} parameter is weaker in the thiospinel. For $U_{eff}=1$ eV the band structure calculations show greigite to be a semimetal, with the minority-spin band of the Fe octahedral sites providing charge carriers at the Fermi level. Further experimental investigations would be necessary in order to test this prediction.

Simulations of the theoretical monoclinic structure of greigite, based on the low-temperature magnetite structure, have shown that this form is not energetically favorable compared to the spinel structure for any U_{eff} values between 0 and 5 eV, indicating that greigite should not experience any Verwey-type transition to a monoclinic structure at low temperatures. While the mechanics of the Verwey transition are still an open area of research with many unanswered questions, previous *ab initio* calculations[36] have highlighted the importance of electron correlations in the transition, represented by a U_{eff} correction of around 3.2 eV or greater. Our calculations have shown that the stabilization of the monoclinic greigite structure with respect to the spinel would require unrealistically high values of $U_{eff} > 5$ eV. Since it has been shown in this study that an accurate description of greigite is provided by a much lower U_{eff} value of 1 eV, it is postulated that the electron correlation associated with the Fe atoms in greigite is insufficient to facilitate a Verwey-type transition.

The finding that greigite is a ferrimagnetic semimetal, which conducts in only one spin polarization, places greigite within a very select group of materials with important applications in the field of spintronics,[56] which could be particularly relevant since iron sulfides offer scope for doping af other manipulations not possible in oxides.[57] In addition, greigite offers a much better example of a low-temperature iron spinel than magnetite, since it does not undergo a phase transformation at low temperature.

ACKNOWLEDGMENTS

Via our membership of the U.K.'s HPC Materials Chemistry Consortium, which is funded by EPSRC-GB (Contract No. EP/F067496), this work made use of the facilities of HECToR, the U.K.'s national high-performance computing service, which is provided by UoE HPCx Ltd at the University of Edinburgh, Cray Inc. and NAG Ltd, and funded by the Office of Science and Technology through EPSRC-GB's High End Computing Programme. We also thank the EPSRC-GB for financial support; the use of the Chemical Database Service at Daresbury.

*a.devey@ucl.ac.uk

[1] I. Letard, Ph. Sainctavit, N. Menguy, J.-P. Valet, A. Isambert, M. Dekkers, and A. Gloter, Phys. Scr., **T115**, 489 (2005).
[2] B. J. Skinner, R. C. Erd, and F. S. Grimaldi, Am. Mineral. **49**, 543 (1964).
[3] A. P. Roberts and R. Weaver, Earth Planet. Sci. Lett. **231**, 263 (2005).
[4] M. J. Dekkers, H. F. Passier, and M. A. A. Schoonen, Geophys. J. Int. **141**, 809 (2000).
[5] M. J. Russell and A. J. Hall, J. Geol. Soc. (London) **154**, 377 (1997).
[6] N. N. Nair, E. Schreiner, R. Pollet, V. Staemmler, and D. Marx, J. Chem. Theory Comput. **4**, 1174 (2008).
[7] S. K. Goffredi, A. Warén, V. J. Orphan, C. L. Van Dover, and R. C. Vrijenhoek, Appl. Environ. Microbiol. **70**, 3082 (2004).
[8] M. Pósfal, P. R. Buseck, D. A. Bazylinski, and R. B. Frankel, Am. Mineral. **83**, 1469 (1998).
[9] A. R. Lennie, S. A. T. Redfern, P. E. Champness, C. P. Stoddart, P. F. Schofield, and D. J. Vaughan, Am. Mineral. **82**, 302 (1997).
[10] A. R. Lennie, S. A. T. Redfern, P. F. Schofield, and D. J. Vaughan, Miner. Mag. **59**, 677 (1995).
[11] Z. He, S.-H. Yu, X. Zhou, X. Li, and J. Qu, Adv. Funct. Mater. **16**, 1105 (2006).
[12] W. Han and M. Gao, Cryst. Growth Des. **8**, 1023 (2008).
[13] M. Uda, Am. Mineral. **50**, 1487 (1965).
[14] M. R. Spender, J. M. D. Coey, and A. H. Morrish, Can. J. Phys. **50**, 2313 (1972).
[15] L. Chang, A. Roberts, Y. Tang, B. D. Rainford, A. R. Muxworthy, and Q. Chen, J. Geophys. Res. **113**, B06104 (2008).
[16] R. Aragón, Phys. Rev. B **46**, 5328 (1992).
[17] D. J. Vaughan and M. S. Ridout, J. Inorg. Nucl. Chem. **33**, 741 (1971).
[18] R. E. Vandenberghe, E. de Grave, P. M. A. De Bakker, M. Krs, and J. J. Hus, Hyperfine Interact. **68**, 309 (1991).
[19] T. Zemčík and A. Cimbálníková, Hyperfine Interact. **83**, 499 (1994).
[20] J. A. Morice, L. V. C. Rees, and D. T. Rickard, J. Inorg. Nucl. Chem. **31**, 3797 (1969).
[21] M. Uhl and B. Siberchicot, J. Phys.: Condens. Matter **7**, 4227 (1995).
[22] S. Sasaki, Acta Crystallogr. **B53**, 762 (1997).
[23] J. M. D. Coey, M. R. Spender, and A. H. Morrish, Solid State Commun. **8**, 1605 (1970).
[24] B. M. Moskowitz, R. B. Frankel, and D. A. Bazylinski, Earth

Planet. Sci. Lett. **120**, 283 (1993).
[25] A. P. Roberts, Earth Planet. Sci. Lett. **134**, 227 (1995).
[26] V. I. Anisimov, F. Aryasetiawan, and A. I. Liechtenstein, J. Phys.: Condens. Matter **9**, 767 (1997).
[27] H. P. Pinto and S. D. Elliot, J. Phys.: Condens. Matter **18**, 10427 (2006).
[28] G. Kresse and J. Hafner, Phys. Rev. B **47**, 558 (1993).
[29] G. Kresse and J. Hafner, Phys. Rev. B **49**, 14251 (1994).
[30] G. Kresse and J. Furthmuller, Comput. Mater. Sci. **47**, 558 (1996).
[31] G. Kresse and J. Furthmuller, Phys. Rev. B **54**, 11169 (1996).
[32] M. C. Payne, M. P. Teter, D. C. Allan, T. A. Arias, and J. D. Joannopoulos, Rev. Mod. Phys. **64**, 1045 (1992).
[33] D. Hobbs and J. Hafner, J. Phys.: Condens. Matter **11**, 8197 (1999).
[34] A. Rohrbach, J. Hafner, and G. Kresse, J. Phys.: Condens. Matter **15**, 979 (2003).
[35] A. Devey, R. Grau-Crespo, and N. H. de Leeuw, J. Phys. Chem. C **112**, 10960 (2008).
[36] P. Piekarz, K. Parlinski, and A. M. Oles, Phys. Rev. B **76**, 165124 (2007).
[37] L. Marsella and V. Fiorentini, Phys. Rev. B **69**, 172103 (2004).
[38] R. Grau-Crespo, F. Corà, A. A. Sokol, N. H. de Leeuw, and C. R. A. Catlow, Phys. Rev. B **73**, 035116 (2006).
[39] A. Walsh, S.-H. Wei, Y. Yan, M. M. Al-Jassim, J. A. Turner, M. Woodhouse, and B. A. Parkinson, Phys. Rev. B **76**, 165119 (2007).
[40] J. P. Perdew, J. A. Chevary, S. H. Vosko, K. A. Jackson, M. R. Pederson, D. J. Singh, and C. Fiolhais, Phys. Rev. B **46**, 6671 (1992).
[41] S. H. Vosko, L. Wilk, and M. Nusair, Can. J. Phys. **58**, 1200 (1980).
[42] P. E. Blöchl, Phys. Rev. B **50**, 17953 (1994).
[43] G. Kresse and D. Joubert, Phys. Rev. B **59**, 1758 (1999).
[44] H. J. Monkhorst and J. D. Pack, Phys. Rev. B **13**, 5188 (1976).
[45] N. D. Mermin, Phys. Rev. **137**, A1441 (1965).
[46] F. Zhou, M. Cococcioni, K. Kang, and G. Ceder, Electrochem. Commun. **6**, 1144 (2004).
[47] X. Du, Q. Li, H. Su, and J. Yang, Phys. Rev. B **74**, 233201 (2006).
[48] G. Rollmann, P. Entel, A. Rohrbach, and J. Hafner, Phase Transitions **78**, 251 (2005).
[49] A. I. Liechtenstein, V. I. Anisimov, and J. Zaanen, Phys. Rev. B **52**, R5467 (1995).
[50] S. L. Dudarev, G. A. Botton, S. Y. Savrasov, C. J. Humphreys, and A. P. Sutton, Phys. Rev. B **57**, 1505 (1998).
[51] I. V. Solovyev, P. H. Dederichs, and V. I. Anisimov, Phys. Rev. B **50**, 16861 (1994).
[52] A. Sorkin, M. A. Iron, and D. G. Truhlar, J. Chem. Theory Comput. **4**, 307 (2008).
[53] O. A. Vydrov, J. Heyd, A. V. Krukau, and G. E. Scuseria, J. Chem. Phys. **125**, 074106 (2006).
[54] R. F. W. Bader, M. T. Carroll, J. R. Cheeseman, and C. Chang, J. Am. Chem. Soc. **109**, 7968 (1987).
[55] J. P. Wright, J. P. Attfield, and P. G. Radaelli, Phys. Rev. B **66**, 214422 (2002).
[56] S. A. Wolf, D. D. Awschalom, R. A. Burhman, J. M. Daughton, S. von Molnár, M. L. Roukes, A. Y. Chtchelkanova, and D. M. Treger, Science **294**, 1488 (2001).
[57] M. I. Katsnelson, V. Yu. Irkhin, L. Chioncel, A. I. Lichtenstein, and R. A. de Groot, Rev. Mod. Phys. **80**, 315 (2008).